Neuron
Article

Purkinje Cells in Posterior Cerebellar Vermis Encode Motion in an Inertial Reference Frame

Tatyana A. Yakusheva,[1] Aasef G. Shaikh,[1] Andrea M. Green,[1,3] Pablo M. Blazquez,[2] J. David Dickman,[1] and Dora E. Angelaki[1,*]
[1] Department of Anatomy and Neurobiology
[2] Department of Otolaryngology
Washington University School of Medicine, St. Louis, MO 63110, USA
[3] Present address: Département de Physiologie, Université de Montréal, Montréal, QC H3C 3J7, Canada.
*Correspondence: angelaki@pcg.wustl.edu
DOI 10.1016/j.neuron.2007.06.003

SUMMARY

The ability to orient and navigate through the terrestrial environment represents a computational challenge common to all vertebrates. It arises because motion sensors in the inner ear, the otolith organs, and the semicircular canals transduce self-motion in an egocentric reference frame. As a result, vestibular afferent information reaching the brain is inappropriate for coding our own motion and orientation relative to the outside world. Here we show that cerebellar cortical neuron activity in vermal lobules 9 and 10 reflects the critical computations of transforming head-centered vestibular afferent information into earth-referenced self-motion and spatial orientation signals. Unlike vestibular and deep cerebellar nuclei neurons, where a mixture of responses was observed, Purkinje cells represent a homogeneous population that encodes inertial motion. They carry the earth-horizontal component of a spatially transformed and temporally integrated rotation signal from the semicircular canals, which is critical for computing head attitude, thus isolating inertial linear accelerations during navigation.

INTRODUCTION

Orienting and navigating relative to the world, both of which constitute fundamental tasks that we experience daily, pose an important computational challenge: sensory information (visual, vestibular, somatosensory) is typically encoded in a local (e.g., eye, head) reference frame. Terrestrial life, however, depends on an allocentric (inertial) reference frame that is often defined by the force of gravity. As a result, a set of either implicit or explicit reference frame transformations is necessary for both spatial perception and sensorimotor transformations. Coding of space in allocentric coordinates has been suggested (Dean and Platt, 2006; Fitzpatrick et al., 2006; Van Pelt et al., 2005), yet the neural signature of these behavioral observations has remained obscure.

Important sensory information about our motion and orientation relative to the world arises from labyrinthine receptors in the inner ear. However, interpretation of signals from the peripheral vestibular sensors, the semicircular canals and the otolith organs, faces two interdependent problems (Figures 1A and 1B). The first, referred to as the "*reference frame problem*," arises because vestibular sensors are physically fixed in the head. Thus, during rotation primary semicircular canal afferents detect endolymph fluid motion relative to the bony ducts, coding angular velocity in a head-centered reference frame but providing no information about how the head moves relative to the outside world (Goldberg and Fernandez, 1975). For example, a horizontal (yaw) rotation in upright orientation activates semicircular canal afferents similar to a yaw rotation in supine orientation (Figure 1A). Yet these two movements differ in inertial (earth-centered) space. The second, referred to as the "*linear acceleration problem*," is due to a sensory ambiguity that arises because of physical laws (Einstein's equivalence principle). As a result, otolith afferents detect net linear acceleration but cannot distinguish translational from gravitational components (Figure 1B; Fernandez and Goldberg, 1976a). As a result, displacement to the right activates otolith afferents similarly as a leftward tilt.

The brain thus faces the task of computing inertial motion and spatial orientation using multimodal integration. In general, visual, somatosensory and efference copies of the motor command signals can provide useful cues for supplementing vestibular afferent activity during navigation. However, even in the absence of these extravestibular cues (e.g., during passive motion in darkness), a solution to both of these computational problems can be achieved by combining signals from the two vestibular sensors (see the Supplemental Data available with this article online; see also Angelaki et al., 1999; Glasauer and Merfeld, 1997; Green and Angelaki, 2004; Green et al., 2005; Merfeld and Zupan, 2002; Zupan et al., 2002). Recent neurophysiological studies have suggested that labyrinthine-receiving areas in the vestibular (VN) and cerebellar (fastigial, FN) nuclei carry convergent otolith

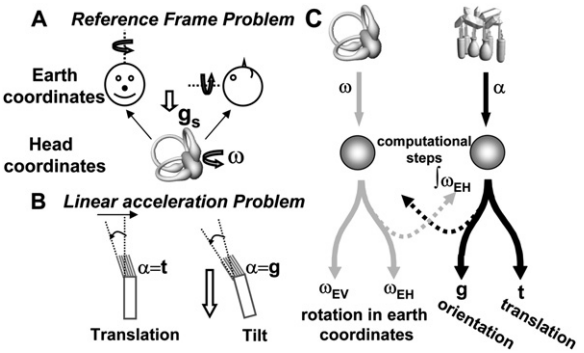

Figure 1. Schematics Illustrating the "Reference Frame" and "Linear Acceleration" Problems, along with the Proposed Mathematical Solution

(A) The "Reference frame" problem is illustrated by an example of two yaw rotations that are identical in head coordinates but differ in earth-centered coordinates. Yaw rotations in upright and supine orientations differ relative to the direction of gravity (g_s, defining here the earth reference frame), yet elicit identical semicircular canal afferent responses that encode rotation, ω, in head-centered coordinates.

(B) The "Linear acceleration" problem is described by schematizing that hair cells and otolith afferents encode net linear acceleration, α, thus respond identically to either translational, t, or gravitational, g, components.

(C) Proposed computational solution, schematized as two steps (for details about the underlying mathematics, see Supplemental Data). To solve the "Reference frame" problem, neural estimates of g must be used by the brain to decompose the head-fixed canal activation, ω, into earth-vertical (ω_{EV}, parallel to gravity) and earth-horizontal (ω_{EH}, perpendicular to gravity) components. To solve the "Linear acceleration" problem, a change in angular orientation can be computed by temporal integration of ω_{EH}. This signal ($\int\omega_{EH}$) can then be combined with net linear acceleration from otolith afferents to extract translation.

and semicircular canal signals that could provide a population solution to the inertial motion detection problem (Angelaki et al., 2004; Green et al., 2005; Shaikh et al., 2005a). However, little is currently known about where this decoding takes place or whether and how spatially transformed signals are represented in the firing rates of individual neurons.

Here we explore the hypothesis that inertial motion is explicitly coded by single Purkinje cells in the cortex of the nodulus (lobule 10) and uvula (lobule 9; collectively referred to as NU), areas that receive direct primary vestibular afferent inputs and are heavily interconnected with the VN (Barmack, 2003; Naito et al., 1995; Newlands et al., 2003). We report that, unlike vestibular and cerebellar nuclei neurons, where a mixture of responses was observed, NU Purkinje cells comprise a homogeneous population that encodes inertial motion. Consistent with recent computational model predictions (Green and Angelaki, 2004), we also show that NU Purkinje cells carry a spatially transformed and temporally integrated rotation signal from the semicircular canals that is used to compute head attitude (i.e., angular position in world coordinates). We conclude that the output of the two most posterior lobules of the primate cerebellar vermis reflects an elegant solution to both computational problems (Figures 1A and 1B) necessary for allocentric orientation and inertial navigation.

RESULTS

Computational Solution to Inertial Motion Detection

Several studies have emphasized that a unique mathematical solution to the inertial motion detection problem can exist using exclusively vestibular afferent information (Angelaki et al., 1999; Green and Angelaki, 2003, 2004; Green et al., 2005; Glasauer and Merfeld, 1997; Merfeld, 1995; Merfeld and Zupan, 2002; Mergner and Glasauer, 1999; Zupan et al., 2002). The mathematical solution, schematized in Figure 1C, consists of two interdependent steps (see Supplemental Data for details). First, rotational signals from the semicircular canals (ω, coded in head-centered coordinates) must be processed by a gravity signal to construct an estimate of angular velocity in earth-centered coordinates (Figure 1C, dashed black arrow). Such an interaction can be used to decompose angular velocity into two spatially defined components: an earth-vertical (i.e., parallel to gravity) component, ω_{EV}, and an earth-horizontal (perpendicular to gravity) component, ω_{EH} (Figure 1C, solid gray arrows). Importantly, only the latter, ω_{EH}, signals a change of orientation relative to gravity. As a result, temporal integration of ω_{EH} ($\int\omega_{EH}$) can yield an estimate of spatial attitude or "tilt" (Figure 1C, dashed gray arrow). In a second computational step this tilt signal, $\int\omega_{EH}$, can be combined with net linear acceleration from the otolith organs, α, to extract the linear acceleration component that is due to translation, t (Figure 1C, solid black arrows). Notice that the computational solutions to the two problems facing inertial navigation are not independent, but intimately coupled, as rotational velocity cannot be interpreted in a spatial frame without knowledge of head orientation relative to gravity. Similarly, parsing net linear acceleration into tilt (gravitational) and translational components requires knowledge about the integral of rotational velocity in an earth-centered reference frame (Green and Angelaki, 2004).

Here we have characterized the simple spike responses of NU Purkinje cells during rotational and/or translational motion in darkness to test the hypothesis that they represent the output of the computational steps illustrated in Figure 1C (right). Specifically, we hypothesize that NU Purkinje cells receive signals from both types of vestibular sensors, such that their firing rates selectively encode inertial (translational) motion (t). The schematic diagram of Figure 1C postulates that, for coding translation, NU Purkinje cells must carry not only an otolith-driven signal (α), but also a spatially and temporally transformed semicircular canal signal ($\int\omega_{EH}$). We have organized the results into three sections, testing each of the following hypotheses: (1) NU Purkinje cells encode translation (rather than net linear acceleration like otolith afferents; Fernandez and Goldberg, 1976a); (2) NU Purkinje cells carry a semicircular canal-driven signal that is spatially transformed to reflect solely the earth-horizontal component of rotation

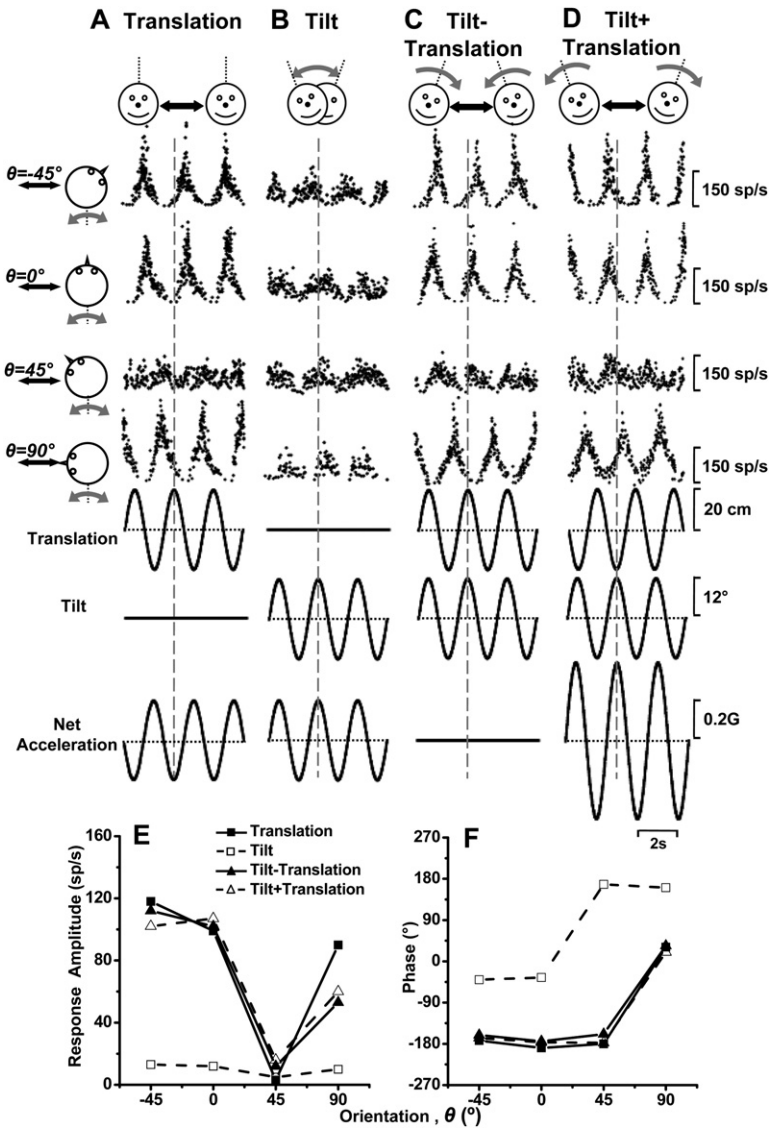

Figure 2. Typical Example of NU Purkinje Cell Responses

(A–D) Instantaneous firing rate of a typical Purkinje cell during Translation (A), Tilt (B), Tilt − Translation (C), and Tilt + Translation (D) (0.5 Hz). Data are shown along four stimulation axes (cartoon drawings), with the translation/tilt position (bottom traces) being matched in both amplitude and direction to elicit an identical net acceleration in the horizontal plane. Straight black and curved gray arrows denote translation and tilt axes of stimulation, respectively. Vertical dotted lines mark the peak stimulus amplitude.

(E and F) Summary of peak firing rate modulation amplitude (E) and phase (F) as a function of stimulus orientation, θ. Data are shown separately for Translation (filled squares, solid lines), Tilt (open squares, dashed lines), Tilt − Translation (filled triangles, solid lines), and Tilt + Translation (open triangles, dashed lines).

(i.e., that which changes head orientation relative to gravity); and (3) this canal-driven, spatially transformed signal has also been temporally integrated, thus coding head position relative to gravity (rather than rotational velocity, as do semicircular canal afferents; Fernandez and Goldberg, 1971).

Purkinje Cells Encode Translation Rather Than Net Linear Acceleration

To test whether NU Purkinje cells selectively encode translation and ignore changes in head orientation relative to gravity (i.e., tilting movements that activate otolith afferents similarly as translation), we recorded neural activities during combinations of sinusoidal (0.5 Hz) tilt (rotation) and translation stimuli (Angelaki et al., 1999, 2004). The peak amplitude of the sinusoidal tilt was adjusted to produce a 0.5 Hz linear acceleration component (due to changes in head orientation relative to gravity) that was the same (0.2 G) as that during translation. The tilt and translation motions were delivered either in isolation (Figures 2A and 2B) or together (Figures 2C and 2D). To facilitate interpretation of cell responses during tilt, translation, and their combinations, net linear acceleration (the stimulus encoded by otolith afferents; Fernandez and Goldberg, 1976a, 1976b) has also been plotted in Figures 2A–2D ("Net Acceleration" traces).

Combination stimuli differed in terms of the relative directions of tilt and translation (i.e., the relative phase of the two sinusoidal movements). Whenever a head tilt to the right occurred simultaneously with translation to the left, gravitational and inertial accelerations were oppositely directed and, if appropriately matched in amplitude, canceled out, and neither component was transduced to the brain (Figure 2C; "Tilt − Translation"). This occurs because during Tilt − Translation net acceleration is zero, and otolith afferents cease to modulate (Angelaki

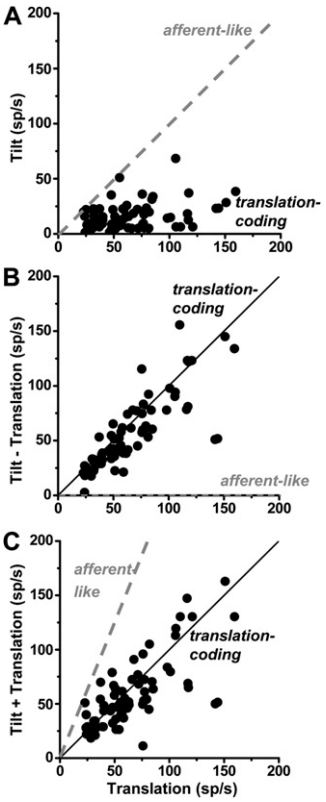

Figure 3. Summary of Purkinje Cell Responses

Summary of neural responses during Tilt (A), Tilt − Translation (B), and Tilt + Translation (C), plotted as a function of the corresponding response during Translation (0.5 Hz) (n = 72). Dashed gray and solid black lines illustrate the predictions for "afferent-like" and "translation-coding" neurons, respectively.

et al., 2004). In contrast, whenever a head tilt to the right occurred simultaneously with translation to the right, the two accelerations summed, resulting in net linear acceleration that was double that for each movement alone (Figure 2D; "Tilt + Translation"). Unlike otolith afferent responses, a cell that selectively encodes translation should modulate similarly during Translation, Tilt − Translation, and Tilt + Translation, with little or no modulation during Tilt (Figures 2A–2D, "Translation" traces).

The top rows of Figures 2A and 2B illustrate the simple spike responses from a typical Purkinje cell. Each row plots responses during motion along one of four directions spaced 45° apart, including lateral translation/roll tilt (θ = 0°; 2nd row) and fore-aft translation/pitch tilt (θ = 90°; 4th row). In contrast to otolith afferents (Figures 2A–2D, "Net Acceleration" traces), the amplitude of NU Purkinje cell responses was large during translation but small during tilt (compare peak-to-trough sinusoidal modulation of firing rate in Figures 2A and 2B). Peak response modulation during translation varied according to the cosine of the angle between the motion direction and the cell's preferred direction (Figure 2E, solid squares and solid line). Also, typical of cosine-like tuning, response phase (i.e., timing of peak neural response relative to stimulus peak) shifted ~180° for motion directions on either side of the minimum response direction that occurred at θ = 45° (Figure 2F, solid squares and solid line). In contrast, tilt responses were small for all stimulus directions (Figure 2E, open squares and dashed line) despite an identical net linear acceleration stimulus to otolith afferents. Similar conclusions were also made when translation and tilt were presented simultaneously: responses during Tilt + Translation and Tilt − Translation were similar to those during Translation (Figures 2C–2F, compare triangles versus solid squares).

Peak response amplitudes from 72 Purkinje cells have been summarized in Figure 3. Responses to tilt were significantly attenuated compared to those during translation [repeated measures ANOVA, $F(1,71) = 171$, $p << 0.001$]. In contrast to the "afferent-like" prediction (i.e., identical responses to tilt and translation; Figure 3A, unity-slope dashed line), most data fell close to the abscissa, as expected for neurons selectively responsive to translation (Figure 3A, "translation-coding" prediction; solid line parallel to abscissa). Similar conclusions were also drawn from the combined stimuli (Figures 3B and 3C). There was a significant correlation between responses to the combined stimuli and those during translation, with slopes of 1.00 (95% confidence interval: [0.81, 1.24], $r = 0.86$, $p << 0.001$) and 0.99 (95% confidence interval: [0.73, 1.19], $r = 0.76$, $p << 0.001$) for Tilt − Translation and Tilt + Translation, respectively. These slopes were thus indistinguishable from unity ("translation-coding" predictions; Figures 3B and 3C, solid black lines) and different from a slope of 0 or 2 ("afferent-like" predictions; Figures 3B and 3C, dashed lines). For all stimuli, the cells appeared to selectively modulate in response to translation but failed to modulate strongly during the tilt movement.

Of particular relevance is the fact that Purkinje cells modulate during Tilt − Translation, although primary otolith afferents do not respond to this stimulus (because the net horizontal plane linear acceleration is zero; Figure 2C, see also Angelaki et al., 2004). Tilt − Translation responses thus reflect an extraotolith signal whose origin was confirmed here to arise from the semicircular canals. In particular, after surgical inactivation (plugging) of all six semicircular canals, Purkinje cell modulation in the Tilt − Translation condition decreased significantly from that in labyrinthine-intact animals (Student's t test, $t_{89} = 6.7$; $p << 0.001$). This is illustrated in Figure 4, which plots responses from a typical Purkinje cell after canal plugging. The format is similar to that of Figure 2, illustrating cell responses from two stimulus directions, lateral translation/roll tilt (θ = 0°; 1st row) and fore-aft translation/pitch tilt (θ = 90°; 2nd row). Notably, despite a clear modulation during Translation (Figure 4A), Tilt − Translation elicited little modulation (Figure 4C). Unlike the pattern of responses in labyrinth-intact animals, which followed that of "Translation" (Figures 2A–2D), Purkinje cell responses after canal plugging followed net acceleration (Figures 4A–4D). Accordingly, they modulated similarly

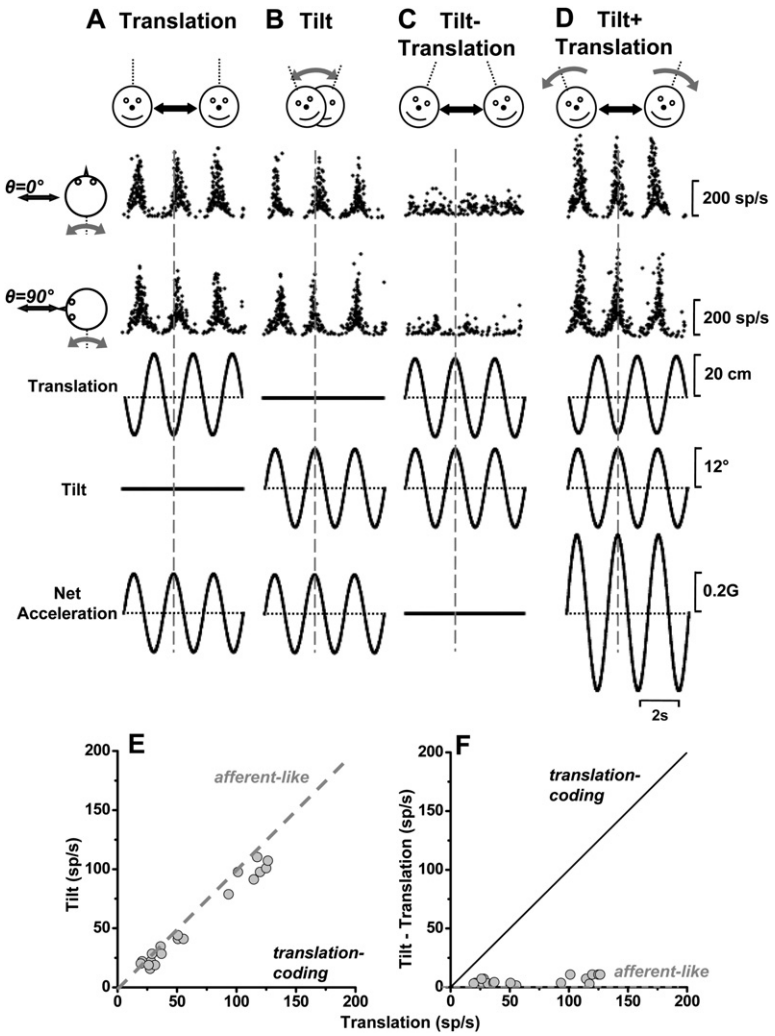

Figure 4. Data after Canal Plugging

(A–D) Instantaneous firing rate of a typical Purkinje cell during Translation, Tilt, Tilt − Translation, and Tilt + Translation (0.5 Hz). Same format as in Figures 2A–2D.

(E and F) Summary of neural responses during Tilt and Tilt − Translation plotted as a function of the corresponding response during Translation (n = 19). Dashed gray and solid black lines illustrate the predictions for "afferent-like" and "translation-coding" neurons, respectively.

during Translation and Tilt but did not modulate during Tilt − Translation.

These data are summarized for 19 Purkinje cells in canal-plugged animals in Figures 4E and 4F. Like otolith afferents but unlike responses in intact animals, responses to Tilt and Translation were similar [repeated measures ANOVA, $F(1,36) = 0.64$, $p = 0.43$], with a correlation slope of 0.9, indistinguishable from unity (95% confidence interval: [0.71, 1.13], $r = 0.98$, $p << 0.001$; Figure 4E). In addition, unlike the predictions for translation-coding neurons, Tilt − Translation versus Translation data fell close to the abscissa, as expected for afferent-like neurons encoding net acceleration (Figure 4F). The ratio of Tilt − Translation to Translation responses decreased from 0.78 ± 0.14 in normal animals to 0.10 ± 0.07 after canal plugging.

The observations in Figures 3 and 4 were further quantified using a partial correlation analysis in which the responses of each cell to all four stimuli (Translation, Tilt, Tilt + Translation, and Tilt − Translation) were simultaneously fitted with "afferent-like" and "translation-coding" models (see Experimental Procedures). To simplify plotting and visual interpretation, the variances of these partial correlation coefficients were normalized using Fisher's r-to-z transform (Angelaki et al., 2004; Smith et al., 2005). Figure 5A plots the z-transformed partial correlation coefficients of the translation model against those of the afferent-like model. Data in the labyrinthine-intact animals fell mostly in the upper left (and none in the lower right) quadrant defined by the dashed lines corresponding to a 0.01 level of significance (Figure 5A, black circles). Thus, Purkinje cells in labyrinthine-intact animals were significantly better fit with the translation-coding as compared to the afferent-like model. The reverse was true after canal inactivation, when translation z scores decreased from 13.4 ± 5.6 to 1.8 ± 1.4 (ANOVA, $p << 0.001$) and data fell in the lower-right quadrant (illustrating significantly better fit with the afferent-like model; Figure 5A, gray-filled symbols). Because canal signals were no longer available to estimate the component of linear acceleration due to changes in head orientation relative to gravity, after canal

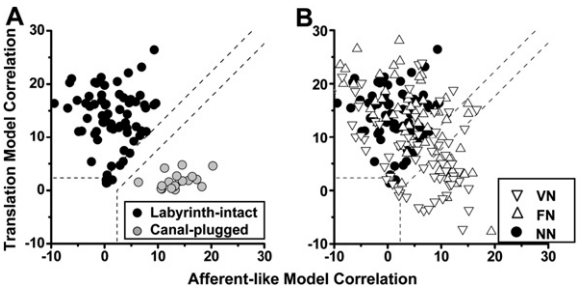

Figure 5. Scatter Plots of z Scores Corresponding to the Partial Correlation Coefficients for Fits of Each Cell Response with the "Translation-Coding" and "Afferent-like" Models

(A) Data from n = 72 cells in labyrinthine-intact (black circles) and n = 19 cells in canal-plugged animals (gray circles) during 0.5 Hz motion stimuli.

(B) NU Purkinje cell data (solid circles) are compared with those previously recorded in VN/FN neurons (open triangles). The superimposed dashed lines divide the plots into three regions: an upper left area corresponding to cell responses that were significantly better fit ($p < 0.01$) by the translation-coding model, a lower right area that includes neurons that were significantly better fit by the afferent-like model, and an in-between area that would include cells that were not significantly better fit by either model. Data shown for the cell's best-responding translation direction.

plugging Purkinje cells responded similarly to tilt and translation.

Thus, by combining signals from both the otolith organs and the semicircular canals, NU Purkinje cell responses reflect the solution of the linear acceleration problem and selectively encode translation. This is consistent with the schematic diagram of Figure 1C, with the vermal cortex conceptually lying within the bottom/right part of the computational scheme. Notably, NU Purkinje cell population z scores differed from those in VN/FN neurons, where data spanned the whole range and many had afferent-like properties [Figure 5B, filled circles versus open triangles; MANOVA, $F(2,206) = 6.0$, $p = 0.003$; Angelaki et al., 2004].

The conceptual diagram of Figure 1C also recapitulates that canal signals on Purkinje cells should have been processed relative to canal afferent information in two important aspects (Green and Angelaki, 2004; see also Supplemental Data): First, the canal-driven component of Purkinje cell responses should be in an earth-centered (as opposed to a head-centered) reference frame. Second, it should also be temporally integrated, thus reflecting a tilt position (i.e., angular orientation) rather than an angular velocity signal. Using Purkinje cell responses during Tilt – Translation, we next investigate each of these predictions. Note that we used Tilt – Translation to investigate these predictions because it is only during this motion that the dynamic acceleration stimulus to the otoliths is zero, and Purkinje cell modulation arises exclusively from semicircular canal activation (as shown after canal plugging in Figure 4).

Purkinje Cell Responses to Earth-Vertical and Earth-Horizontal Axis Rotations: Evidence for Reference Frame Transformation of Canal Signals

To appreciate the expected differences in firing rates based on an earth-centered or head-fixed reference frame, let's revisit the example cell in Figure 2. During earth-horizontal axis rotations, this cell carried a vertical canal-borne signal with a preferred direction halfway between roll and pitch (Figure 2C, "Tilt – Translation" stimulus; a rotation is described as "earth-horizontal" or "earth-vertical" based on the relative orientation of the rotation axis and gravity; see Experimental Procedures). If this canal-driven signal is afferent-like in the sense that it encodes rotation in a head-fixed reference frame (signal ω in Figure 1C), responses should be independent of the spatial orientation of the rotation axis relative to gravity. Accordingly, the cell of Figure 2 should also modulate similarly during earth-vertical axis rotations that activate the vertical semicircular canals (e.g., roll responses in upright orientation should be the same as roll responses in supine orientation). In contrast, if Purkinje cells selectively encode only the earth-horizontal rotational component, ω_{EH} (as hypothesized in the scheme of Figure 1C), they should not modulate at all during earth-vertical axis rotations.

That the latter was indeed the case is shown in Figures 6A–6C, which plots earth-vertical axis rotation responses from the same example cell as in Figure 2. There was no stimulus-driven sinusoidal modulation during rotation with the animal either upright (Figure 6A; when mainly the horizontal semicircular canals were stimulated) or tilted by as much as ±45° (Figures 6B and 6C; when not only the horizontal but also the vertical semicircular canals were stimulated). Such absence of modulation during vertical canal stimulation (either in roll [Figure 6B] or pitch [Figure 6C]) when the rotation axis was earth-vertical contrasts with the robust responses seen during roll/pitch oscillations observed during the Tilt – Translation protocol when the axis of rotation was earth-horizontal (Figure 2C).

Figure 6D summarizes these results. Here, peak response modulation during earth-vertical axis rotation with the animal statically tilted relative to the rotation axis (thus activating vertical semicircular canals) has been plotted as a function of the response that would have been predicted if neurons encoded canal information in a head-centered reference frame (i.e., under the assumption that the same canal-derived angular velocity is encoded regardless of the relationship between the axis of rotation and gravity). If the canal response component of NU Purkinje cells was afferent-like and expressed in a head-centered reference frame, data points should have fallen along the unity-slope, dashed line ("Head coordinates"). In contrast, as illustrated in Figure 6D, data fell near the abscissa ("Earth coordinates") and were significantly lower than the corresponding predictions for a head-centered estimate [ANOVA with repeated measures, $F(1,62) = 101$, $p << 0.001$]. Thus, Purkinje cells selectively encode the earth-horizontal component of semicircular canal afferent activation, a spatially

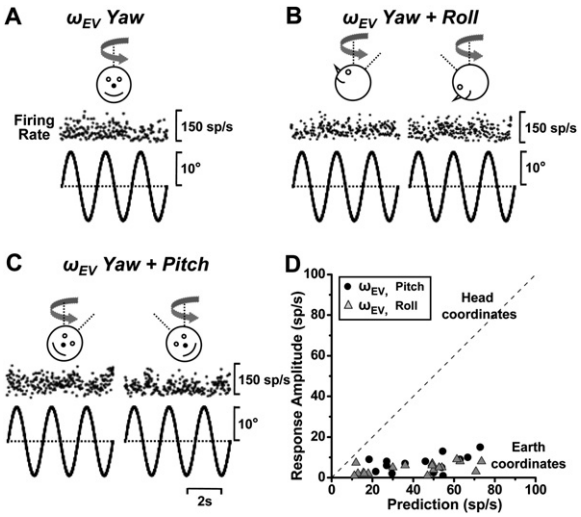

Figure 6. Canal-Driven Responses of Purkinje Cells Encode Rotation in an Earth-Centered Reference Frame

(A–C) Instantaneous firing rate of the Purkinje cell of Figure 2 during earth-vertical axis rotation (coding of ω_{EV}) with the monkey either upright ([A], Yaw rotation) or statically tilted ±45°, bringing the plane of rotation half-way between yaw and roll (B) or pitch (C) (see cartoon drawings).

(D) Peak response modulation during earth-vertical axis rotation with the animal tilted ±30° and/or ±45° (as in [B] and [C]) plotted as a function of the corresponding prediction under the assumption that Purkinje cells encode rotation in a head-centered reference frame. If cerebellar neurons encode rotation in head coordinates, data should fall along the unity slope, dashed line ("head coordinates"). Alternatively, if they selectively modulate only during earth-horizontal (but not earth-vertical) axis rotation, data should fall along the abscissa ("earth coordinates").

transformed signal necessary for inertial motion detection. Next we describe the temporal properties of this component.

Purkinje Cell Responses to Earth-Horizontal Axis Rotations: Evidence for Distributed Temporal Integration

The second prediction from the computational scheme of Figure 1C is that the canal-driven component of Purkinje cell responses should be temporally integrated, thus reflecting a tilt position (i.e., angular orientation) rather than an angular velocity signal. Because our stimulus was not a transient displacement but a sinusoidal motion, responses at a single frequency cannot specify whether cell firing rate follows velocity (like canal afferents) or position (as predicted from the computational scheme of Figure 1C). To test whether Purkinje cells encode angular velocity or its integral, responses at different frequencies need to be characterized. How peak modulation and phase vary with frequency can then be used to distinguish the temporal properties of these responses.

Specifically, if the canal-driven Purkinje cell responses encode angular velocity, velocity gains (computed as the ratio of peak cell modulation amplitude relative to peak stimulus velocity) should be independent of frequency (Fernandez and Goldberg, 1971). Similarly, the phase of velocity-coding neurons should be 0°. In contrast, if the canal-driven response component of NU Purkinje cells encodes angular position, velocity gains should decrease with unity slope as a function of frequency. Equivalently, position gains (computed as modulation amplitude relative to peak stimulus position) should be independent of frequency. To encode tilt position, the phase difference between response and stimulus velocity should be −90° across all frequencies.

Figures 7A and 7B plot velocity and position gains as a function of frequency (0.16, 0.5, and 1 Hz). Velocity gains decreased with frequency, with a slope of −1, which was indistinguishable from unity (CI = [−1.12, −0.88], r = −0.73; p << 0.001), the signature of temporal integration. In contrast, position gains were independent of frequency [Figure 7B, dashed lines; repeated measures ANOVA, F(2,57) = 1.8, p = 0.19]. Response phase (re velocity) was also independent of frequency [repeated measures ANOVA, F(2,57) = 2.6, p = 0.16] and on average close to −90°, compatible with temporal integration. Yet the canal-driven response components of individual NU Purkinje cells were nevertheless characterized by phases that spanned a broad range. Next we explain why such a cell-to-cell variability in response phase is required for the detection of inertial motion.

Spatiotemporal Matching of Convergent Signals

To understand this spread of response phase, we need to revisit the rationale behind these predictions. In the simplified scheme of Figure 1C, a temporal integration would be necessary to convert angular velocity into position (i.e., an angular orientation or tilt signal approximately proportional to the gravitational acceleration for small tilt angles; see Supplemental Data and Green and Angelaki, 2004). During tilt such canal-driven angular position signals would then "cancel" the gravitational component of the otolith afferent response coding net acceleration. An implicit assumption here is that the otolith-driven responses of NU Purkinje cells, like primary otolith afferents, encode linear acceleration. However, several studies have shown that central responses also encode linear velocity and in general exhibit a broad distribution of phase relationships relative to linear acceleration (Angelaki and Dickman, 2000; Angelaki et al., 2004; Chen-Huang and Peterson, 2006; Green et al., 2005; Musallam and Tomlinson, 2002; Shaikh et al., 2005b).

This property, which is generally thought to reflect spatiotemporal convergence and the distributed nature of the temporal processing required to distinguish tilt and translation (Angelaki and Dickman, 2000; Green and Angelaki, 2004), has been illustrated for NU Purkinje cells in Figure 8A. The plot shows the 0.5 Hz phase relationship between the canal-driven (Tilt − Translation) and otolith-driven (Translation) response components for each NU Purkinje cell. Unlike primary otolith afferents, where 0.5 Hz phases are tightly clustered (Fernandez and

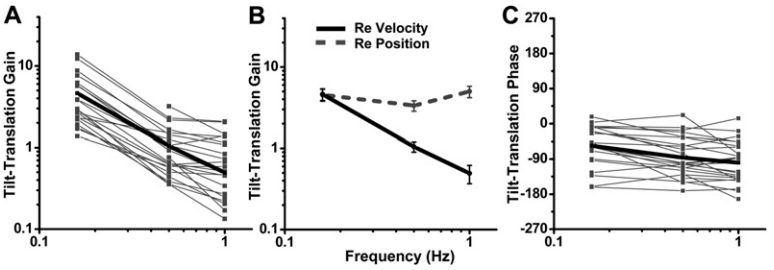

Figure 7. Evidence for Temporal Integration of Canal-Driven Signals

Purkinje cell gain (A and B) and phase (C) during the Tilt − Translation stimulus condition (i.e., isolating the canal-driven response component) plotted as a function of frequency. Gain (in spikes/s per degree/s) and phase (in degrees) in (A) and (C) are expressed relative to the head velocity stimulus. Thin lines and symbols illustrate data from single neurons tested at different frequencies (n = 23; shown only for best-responding stimulus direction); thick lines indicate population averages. (B) shows the mean (±SD) of velocity and position gains (solid black and dashed gray lines, respectively). Velocity gains are expressed in units of spikes/s per degree/s. Position gains are expressed in spikes/s per degree.

Goldberg, 1976b; Angelaki and Dickman, 2000), the phase of the otolith-driven response component in NU Purkinje cells varied widely from cell to cell. The canal-driven component also varied accordingly such that it matched the corresponding otolith-driven response on a cell-by-cell basis (paired Student's t test, $t_{72} = 2.0$; $p = 0.04$). The large cell-to-cell variability in canal-driven response phase illustrated in Figure 7C can thus be explained by the requirement to temporally match canal- and otolith-derived signals on cells that extract inertial motion information.

Finally, the semicircular canal and otolith signal contributions to Purkinje cell firing should not only be temporally but also spatially matched. This was indeed the case, as illustrated in Figure 8B, which plots the distribution of angular differences in preferred direction between the canal-driven (Tilt − Translation) and otolith-driven (Translation) signal components. Preferred response orientations were computed by fitting a spatiotemporal model (Angelaki, 1991; Green et al., 2005) to spatial tuning curves like those in Figures 2E and 2F. The canal and otolith signal contributions to NU Purkinje cells were appropriately matched spatially (preferred direction differences < 30°). These results illustrate that the canal-driven component of Purkinje cell responses provides a temporally and spatially matched complement to the otolith-driven component. This "matched" convergence is a necessary condition for a computational solution to the inertial motion detection problem.

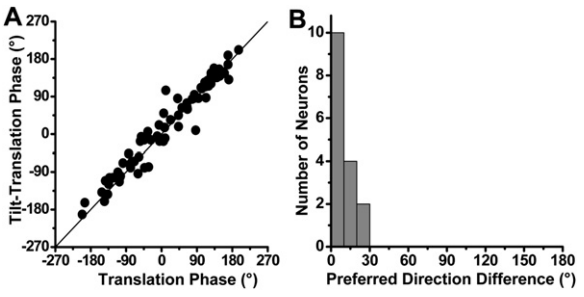

Figure 8. Spatiotemporal Matching of Canal-Driven and Otolith-Driven Signals

(A) Response phase during the 0.5 Hz Tilt − Translation stimulus (canal-driven component) is plotted as a function of the respective phase during Translation (otolith-driven component) (n = 72; data along the best-responding stimulus direction). Phase has been expressed relative to tilt velocity.

(B) Distribution of the difference in preferred directions between the 0.5 Hz Tilt − Translation and Translation stimulus conditions. Data (n = 16) from cells tested at multiple orientations (e.g., Figure 2) and fitted with a spatiotemporal model to compute preferred directions (Angelaki and Dickman, 2000).

DISCUSSION

We have shown here that the simple spike activities of Purkinje cells in the vermal cortex, lobules 10 (nodulus) and 9 (uvula), encode inertial motion and reflect an elegant solution to both computational problems of Figures 1A and 1B. In particular, (1) unlike vestibular and deep cerebellar nuclei neurons, where a mixture of translation-coding and afferent-like responses was observed, NU Purkinje cells seem to comprise a more uniform population that encodes inertial motion. (2) NU Purkinje cells carry a semicircular canal-driven signal that is spatially transformed to reflect solely the earth-horizontal component of rotation (i.e., they only modulate during rotations that change head orientation relative to gravity); and (3) this canal-driven, spatially transformed signal has also been temporally integrated, thus coding head position relative to gravity (rather than rotational velocity as do semicircular canal afferents; Green and Angelaki et al., 2003; Fernandez and Goldberg, 1971). Such an earth-centered estimate of head attitude could then be subtracted from net linear acceleration provided by the otoliths and used to estimate inertial linear accelerations during navigation.

Inertial Navigation: Data and Theory

The role of otolith and semicircular canal cues in inertial motion detection and spatial orientation motivated many pioneering studies (for reviews see Guedry, 1974; Mayne,

1974; Young, 1984). The problem can be summarized as follows. As in man-made inertial guidance systems, inertial self-motion detection involves computation of rotational and translational components expressed relative to an earth-fixed reference. However, because our motion sensors are fixed to the head, they measure the linear acceleration and angular rotation within a reference frame that is head- and not earth-centered (Figures 1A and 1B). As a result, the unprocessed output of the peripheral vestibular sensors neither distinguishes attitude (orientation) from inertial (translational) motion nor signals our true rotation in space (Angelaki et al., 1999; Green and Angelaki, 2004; Green et al., 2005; Glasauer and Merfeld, 1997; Merfeld, 1995; Merfeld and Zupan, 2002; Mergner and Glasauer, 1999; Zupan et al., 2002).

Several behavioral studies have shown that the brain estimates a solution to both computational problems introduced in Figures 1A and 1B. For example, behavioral evidence that the brain can discriminate translational from gravitational accelerations using canal cues has come from both eye movement and perception studies (Angelaki et al., 1999; Green and Angelaki, 2003; Glasauer, 1995; Merfeld et al., 2005a, 2005b; Stockwell and Guedry, 1970). In addition, evidence that the brain computes the earth-referenced components of rotation can be found in both eye movement (Angelaki and Hess, 1994; Angelaki et al., 1995) and perceptual responses (Day and Fitzpatrick, 2005). Notably, after lesion of the NU, reflexive eye movement responses during rotation no longer show evidence for spatial (earth-centered) reference frame transformations (Angelaki and Hess, 1995a; Wearne et al., 1998).

The schematic of Figure 1C (see also Supplemental Data) summarizes the concept of how vestibular signals can be used to solve the inertial motion detection problem. According to these concepts, (1) resolution of both the reference frame and linear acceleration problems implies a convergence of sensory information from the otolith organs and the semicircular canals. (2) The two problems are interdependent. That is, detection of self-rotation relative to the outside world requires an internal neural estimate of gravity. Concurrently, discrimination between an internal estimate of gravity and translational acceleration requires knowledge of the temporal integral of ω_{EH}, emphasizing the functional need for spatially and temporally transformed semicircular canal information. Such spatiotemporally transformed, canal-driven signals (that can be isolated and characterized during Tilt – Translation) are functionally important for computing translation by "eliminating" the component of dynamic otolith afferent activation associated with head reorientations relative to gravity. Here we have shown that NU Purkinje cell activity reflects the output of these transformations.

Role of the NU

The NU has direct projections to the vestibular and fastigial nuclei (Barmack, 2003; Bernard, 1987; Wylie et al., 1994). Several studies, including lesion, neuroanatomical, and single-unit recording experiments, have implicated the cerebellar NU in the central processing of otolith signals (Marini et al., 1975; Fushiki and Barmack, 1997; Ono et al., 2000). In the rabbit, where NU responses have been characterized in detail, both simple and complex spike responses seem to reflect vertical canal and otolith system activation (Barmack and Shojaku, 1995; Fushiki and Barmack, 1997), as well as optokinetic stimulation (Kano et al., 1990a, 1990b, 1991). Here we show that simple spike responses during translation are always larger (often more than 10-fold; Figures 2A and 2B and Figure 3A) than the corresponding tilt responses. Interestingly, although the area receives projections from the horizontal semicircular canals, no Purkinje cell modulation has ever been observed during yaw rotations (see Barmack, 2003 for a review). The scheme in Figure 1C provides an explanation: as long as yaw testing is done in upright orientation (an ω_{EV} stimulus), NU Purkinje cells will not respond, as they carry only the ω_{EH} component of the canal activation. If, however, yaw rotation is delivered in another head orientation (e.g., supine; an ω_{EH} stimulus), we expect that there would be a robust response (Green and Angelaki, 2004; Green et al., 2005).

Finally, although a role of the NU in tilt/translation discrimination has yet to be explored using causal manipulations (e.g., electrical microstimulation or inactivation), there is clear evidence that lesions of the nodulus affect the expression of coordinate transformations of rotation signals during the vestibulo-ocular reflex (Angelaki and Hess, 1995a, 1995b; Barmack et al., 2002; Cohen et al., 1992; Wearne et al., 1998; Wiest et al., 1999). Similar conclusions were reached using electrical stimulation (Heinen et al., 1992; Solomon and Cohen, 1994). Whether these computations occur within the cerebellar cortex itself or through feed-forward and feedback connections with the vestibular and fastigial nuclei remains to be explored. For example, "translation-coding" VN/FN neurons might be the ones connected with the NU, possibly receiving direct projections. Alternatively, the computation can involve the whole circuitry, particularly given the strong interconnectivity between these areas: NU efferents project to VN areas that receive afferents from the contralateral FN (Walberg et al., 1962; Angaut and Brodal, 1967). In addition, NU Purkinje cells regulate the output of NU-projecting VN neurons (Xiong and Matsushita, 2000), and electrical stimulation of the nodulus inhibits vestibulocerebellar pathways (Precht et al., 1976).

Frequency Bandwidth of These Computations: Need for Extravestibular Signals

The effectiveness of semicircular canal signals for the estimation of inertial motion is bandwidth limited. Because of the mechanical properties of the vestibular apparatus, canal afferents do not provide a veridical estimate of angular velocity at low frequencies (Fernandez and Goldberg, 1971). Thus, the ability to discriminate between tilt and translation based solely on vestibular cues (e.g., during passive motion in darkness) deteriorates at low

frequencies (Glasauer, 1995; Kaptein and Van Gisbergen, 2006; Merfeld et al., 2005a, 2005b; Seidman et al., 1998). In fact, it is typically at these low frequencies that perceptual illusions occur ("somatogravic illusion"; Graybiel, 1952; Clark and Graybiel, 1963, 1966; Graybiel et al., 1979; Tormes and Guedry, 1975).

Thus, it is important to emphasize that in general central estimates of inertial motion and spatial orientation are likely to rely on multiple sets of sensorimotor cues including vestibular, visual, and somatosensory signals, as well as efference copies of the motor commands for active movements. Extravestibular rotation cues are likely to be of particular importance at low frequencies (e.g., < 0.1 Hz) or below vestibular detection thresholds (Guedry, 1974). For example, visual rotational cues have been shown to contribute to translational motion estimation (Zupan and Merfeld, 2003; McNeilage et al., 2007), and it is well known that visual cues can significantly influence our percept of head orientation relative to gravity (Dichgans et al., 1972; Howard, 1986; Howard and Hu, 2001). How much each of the sensory cues contributes to inertial motion perception might depend on their relative reliability, as recently shown for statistically optimal multisensory cue integration (e.g., Ernst and Banks, 2002). Visual inputs and efference copy signals may play a large role in solving these computational problems during active navigation. Thus, the fact that a solution is reflected in cerebellar neuron responses during passive motion in darkness is even more surprising. Whether the cerebellar vermis is also involved in multisensory cue integration during active navigation remains to be explored.

EXPERIMENTAL PROCEDURES

Animals and Experimental Setup

Two juvenile fascicularis monkeys (*Maccaca fascicularis*) and one rhesus monkey (*Maccaca mulatta*) were used in this study. The animals were prepared under aseptic conditions and general anesthesia. A circular delrin ring was surgically attached to the skull with stainless steel T bolts and dental acrylic to immobilize the animal's head in the stereotaxic position during recording. A delrin platform with staggered rows of holes was stereotaxically secured inside the head ring. To provide better access to the midline, the platform in two animals was tilted 10° from anterior to posterior and 10° from left to right. All three animals were also chronically implanted with scleral search coils to measure eye movements. After an adequate recovery period, animals were trained to follow a small target light during fixation and pursuit. These behavioral protocols allowed identification of the eye position and velocity sensitivity of cells in the abducens, vestibular, and fastigial nuclei (Angelaki et al., 2004; Dickman and Angelaki, 2002; Shaikh et al., 2005b). The surgical and experimental procedures conformed to the guidelines of the US National Institutes of Health and were approved by the Animal Care and Use Committee at Washington University.

In one animal, neural activities were also collected after bilateral plugging of all six semicircular canals (for details, see Angelaki et al., 1999; Shaikh, et al., 2005a). This was done in one operation by exposing each canal and drilling a small hole in the bony wall of the canal. The membranous duct was then cut with the tip of a sharp knife. Subsequently, the hole was firmly filled with bony chips and covered with a piece of muscle fascia. This procedure does not damage the otolith organs. Data were collected within the first 2 months after surgery. The efficacy of canal plugging was verified by an absent angular vestibulo-ocular reflex (VOR) during 0.5 Hz yaw, pitch, and roll rotations in darkness throughout the period of recordings (the translational VOR was normal).

During experiments the monkeys were comfortably seated in a primate chair secured inside the inner gimbal of a vestibular stimulator composed of a three-axis rotator mounted on a 2 m linear sled (Acutronics Inc., Pittsburgh, PA). The animal was positioned such that all three rotation axes (yaw, pitch, and roll) were aligned with the center of the head and the horizontal stereotaxic plane was aligned with the earth-horizontal. The linear acceleration stimulus was measured by a 3D linear accelerometer attached to the inner frame of the turntable, while angular motion was measured using angular position/rate feedback from the rotator. The eye coil signals and the stimuli were filtered (200Hz; 6-pole Bessel) and digitized at a rate of 833.33 Hz (model 1401, CED, 16-bit resolution; Cambridge Electronics Design, Cambridge, UK).

Neural Recording

NU Purkinje neurons were recorded extracellularly using epoxy-coated tungsten microelectrodes (4–6 MΩ impedance; FHC, Bowdoinham, ME). Each electrode was positioned into a 26-gauge guide tube that was inserted through a predrilled hole in the skull into the cerebellum and advanced using a remote-controlled microdrive. Recorded action potentials were amplified, filtered (300–6 kHz), discriminated with a window-slope trigger, and stored on a computer using the event channel of the 1401 for offline analyses. Neuronal data were also acquired using an analog channel of the 1401 (40 KHz). The data were analyzed offline using Spilke2 (Cambridge Electronic Design) to extract the complex and simple spikes from the raw neuronal data. We sorted spikes based on principal component analysis using a clustering approach.

The nodulus-uvula was identified using stereotaxic coordinates as well as the location of the abducens, vestibular, and fastigial nuclei in each animal (see Figures S1, S2, and S3 for recording locations). Recordings were restricted to the Purkinje cell layer, where both simple and complex spikes could be observed online. All but 15 cells were further identified as Purkinje cells offline using the following criteria: first, simple spikes (SS) and complex spikes (CS) were identified visually by their characteristic waveforms. Second, peri-CS-triggered SS histograms were used to show that SS activity paused for 15 ms after the occurrence of a CS. Because we found no difference in response properties between identified and putative Purkinje cells, the two groups have been considered together in all analyses.

To characterize the properties of NU neurons, the following experimental protocol was delivered in complete darkness. Neural responses were characterized during combinations of tilt and translation stimuli that have been used previously to independently manipulate inertial and net gravitoinertial accelerations (Figure 2; see also Angelaki et al., 1999, 2004). These stimuli consisted of either pure translation (Translation), pure tilt (Tilt), or combined translation and tilt motion stimuli (Tilt − Translation motion and Tilt + Translation motion). The tilt stimulus was a 0.5 Hz sinusoidal rotation from upright with a peak amplitude of 11.3° (36°/s). Because this motion reorients the head relative to gravity, otolith afferents were stimulated by a linear acceleration component in the horizontal plane with a peak magnitude of approximately 0.2 G (G = 9.81 m/s^2). The amplitude of the translation stimulus was adjusted to match that induced by the head tilt (0.2 G, ±20 cm). During combined rotational and translational stimulation, inertial and gravitational acceleration components combined in either an additive or subtractive fashion depending on the relative directions of the two stimuli. As a result, the net gravitoinertial acceleration activating the otolith receptors either doubled (Tilt + Translation) or was nearly zero (Tilt – Translation), even though the actual translation of the animal remained the same.

Each cell was usually characterized at a minimum of two horizontal plane orientations ($\theta = 0°$ and $\theta = 90°$), corresponding to lateral motion/roll tilt and fore-aft motion/pitch tilt, respectively (see

Figures 2A–2D, 2nd and 4th rows). If neural isolation was maintained, this 0.5 Hz protocol was also delivered along two additional directions, half-way in-between the lateral and fore-aft directions ($\theta = -45^\circ$ and $\theta = 45^\circ$; see Figures 2A–2D, 1st and 3rd rows). Along their best-responding direction, several cells were also tested during these four protocols (Translation, Tilt, Tilt − Translation, Tilt + Translation) at two different frequencies, 0.16 Hz (±0.1 G, corresponding to tilt and translation amplitudes of 5.7° and 95.6 cm, respectively) and 1 Hz (±0.087 G, corresponding to tilt and translation amplitudes of 5° and 2.16 cm, respectively). Note that the highest- and lowest-frequency/amplitude parameters were determined by the mechanical limitations of the pitch/roll rotator and sled, respectively.

Finally, a few cells were also tested during earth-vertical axis rotations. Notice that we describe rotations based on their "axis," as defined by the right-hand rule. For example, yaw while upright (rotation axis parallel to gravity) was considered an "earth-vertical axis" rotation, whereas yaw while supine (rotation axis perpendicular to gravity) was considered an "earth-horizontal axis" rotation (Figure 1A). Similarly, pitch/roll while upright were considered "earth-horizontal axis" rotations, whereas pitch/roll while ear-down/supine were considered "earth-vertical axis" rotations. In these experiments, earth-vertical axis rotations (0.5 Hz, ±10°) were delivered with the animal positioned upright, pitched 30° (or 45°) nose-up/down (rotations producing combinations of horizontal and torsional VOR) and rolled 30° (or 45°) right/left ear-down (rotations producing combinations of horizontal and vertical VOR).

Data Analyses

Data analyses were performed offline using Matlab (Mathworks Inc., Natick, MA). Instantaneous firing rate was computed offline as the inverse of interspike interval. Data from multiple cycles of sinusoidal motion were folded into a single cycle by overlaying neural responses. Response amplitude and phase were determined by fitting a sine function to the cumulative responses during each of the translation, tilt, and combined stimuli (Angelaki and Dickman, 2000; Dickman and Angelaki, 2002). Response amplitude refers to half the peak-to-trough modulation, whereas response phase has been expressed relative to translation (or tilt) stimulus velocity.

To determine whether each individual cell encoded translation or net linear acceleration, linear regression analyses were used to simultaneously fit the cumulative cycles of cell modulation during each of the translation, tilt, and combined stimuli using an "afferent-like" and "translation-coding" model. Briefly, these models assume that neural firing rate modulation is either due to the net acceleration or due to the translational acceleration component (for details, see Angelaki et al., 2004; Green et al., 2005). How well each of these two models fitted the data was evaluated using a partial correlation analysis. To remove the influence of correlations between the predictions themselves, we calculated partial correlation coefficients R_A and R_T using the following formulas:

$$R_A = \frac{(r_A - r_T r_{AT})}{\sqrt{(1 - r_T^2)(1 - r_{AT}^2)}}$$

and

$$R_T = \frac{(r_T - r_A r_{AT})}{\sqrt{(1 - r_A^2)(1 - r_{AT}^2)}}$$

where r_A and r_T are the simple correlation coefficients between the data, and each of the model predictions and $r_{AT} = 0.68$ describes the correlation between the two models.

Partial correlation coefficients were subsequently converted to z scores using Fisher's r-to-z transform in order to facilitate the interpretation of statistical significance independently of the number of data points (Angelaki et al., 2004; Smith et al., 2005). The advantage of this comparison is that when z scores for one model are plotted versus the respective z scores for the other model, the plot can be easily separated into regions in which data points can be distinguished as being better correlated with one model as compared to the other at a particular level of significance. Because all NU neurons fell in the upper left quadrant (i.e., reflecting the fact that the translation-coding model provided statistically significant better fits), intermediate models (Angelaki et al., 2004) were not considered here. Correlations between independent variables were obtained by minimizing the perpendicular offset of the data to the line (using a nonlinear least squares algorithm based on the interior-reflective Newton method), with 95% confidence intervals computed using bootstrapping with replacement. Other statistical comparisons of neural responses used analyses of variance and Student's t tests.

Supplemental Data

The Supplemental Data for this article can be found online at http://www.neuron.org/cgi/content/full/54/6/973/DC1/.

ACKNOWLEDGMENTS

The work was supported by grants from NASA (NNA04CC77G) and NIH (F32 DC006540, R01 EY12814). We would like to thank Shawn Newlands for the canal-plugging operation.

Received: February 2, 2007
Revised: May 2, 2007
Accepted: June 5, 2007
Published: June 20, 2007

REFERENCES

Angaut, P., and Brodal, A. (1967). The projection of the "vestibulocerebellum" onto the vestibular nuclei in the cat. Arch. Ital. Biol. *105*, 441–479.

Angelaki, D.E. (1991). Dynamic polarization vector of spatially tuned neurons. IEEE Trans. Biomed. Eng. *11*, 1053–1060.

Angelaki, D.E., and Hess, B.J. (1994). Inertial representation of angular motion in the vestibular system of rhesus monkeys. I. Vestibuloocular reflex. J. Neurophysiol. *71*, 1222–1249.

Angelaki, D.E., and Hess, B.J. (1995a). Inertial representation of angular motion in the vestibular system of rhesus monkeys. II. Otolith-controlled transformation that depends on an intact cerebellar nodulus. J. Neurophysiol. *73*, 1729–1751.

Angelaki, D.E., and Hess, B.J. (1995b). Lesion of the nodulus and ventral uvula abolish steady-state off-vertical axis otolith response. J. Neurophysiol. *73*, 1716–1720.

Angelaki, D.E., and Dickman, J.D. (2000). Spatiotemporal processing of linear acceleration: Primary afferent and central vestibular neuron responses. J. Neurophysiol. *84*, 2113–2132.

Angelaki, D.E., Hess, B.J., and Suzuki, J. (1995). Differential processing of semicircular canal signals in the vestibulo-ocular reflex. J. Neurosci. *15*, 7201–7216.

Angelaki, D.E., McHenry, M.Q., Dickman, J.D., Newlands, S.D., and Hess, B.J. (1999). Computation of inertial motion: Neural strategies to resolve ambiguous otolith information. J. Neurosci. *19*, 316–327.

Angelaki, D.E., Shaikh, A.G., Green, A.M., and Dickman, J.D. (2004). Neurons compute internal models of the physical laws of motion. Nature *430*, 560–564.

Barmack, N.H. (2003). Central vestibular system: Vestibular nuclei and posterior cerebellum. Brain Res. Bull. *60*, 511–541.

Barmack, N.H., and Shojaku, H. (1995). Vestibular and visual climbing fiber signals evoked in the uvula-nodulus of the rabbit cerebellum by natural stimulation. J. Neurophysiol. *74*, 2573–2589.

Barmack, N.H., Errico, P., Ferraresi, A., Fushiki, H., Pettorossi, V.E., and Yakhnitsa, V. (2002). Cerebellar nodulectomy impairs spatial

memory of vestibular and optokinetic stimulation in rabbits. J. Neurophysiol. *87*, 962–975.

Bernard, J.-F. (1987). Topographical organization of olivocerebellar and corticonuclear connections in the rat – An WGA-HRP study: I. Lobules IX, X, and the flocculus. J. Comp. Neurol. *263*, 241–258.

Chen-Huang, C., and Peterson, B.W. (2006). Three dimensional spatial-temporal convergence of otolith related signals in vestibular only neurons in squirrel monkeys. Exp. Brain Res. *168*, 410–426.

Clark, B., and Graybiel, A. (1963). Contributing factors in the perception of the oculogravic illusion. Am. J. Psychol. *76*, 18–27.

Clark, B., and Graybiel, A. (1966). Factors contributing to the delay in the perception of the oculogravic illusion. Am. J. Psychol. *79*, 377–388.

Cohen, H., Cohen, B., Raphan, T., and Waespe, W. (1992). Habituation and adaptation of the vestibuloocular reflex: A model of differential control by the vestibulocerebellum. Exp. Brain Res. *90*, 526–538.

Day, B.L., and Fitzpatrick, R.C. (2005). Virtual head rotation reveals a process of route reconstruction from human vestibular signals. J. Physiol. *567*, 591–597.

Dean, H.L., and Platt, M.L. (2006). Allocentric spatial referencing of neuronal activity in macaque posterior cingulate cortex. J. Neurosci. *26*, 1117–1127.

Dichgans, J., Held, R., Young, L.R., and Brandt, T. (1972). Moving visual scenes influence the apparent direction of gravity. Science *178*, 1217–1219.

Dickman, J.D., and Angelaki, D.E. (2002). Vestibular convergence patterns in vestibular nuclei neurons of alert primates. J. Neurophysiol. *88*, 3518–3533.

Ernst, M.O., and Banks, M.S. (2002). Humans integrate visual and haptic information in a statistically optimal fashion. Nature *415*, 429–433.

Fernandez, C., and Goldberg, J.M. (1971). Physiology of peripheral neurons innervating semicircular canals of the squirrel monkey. II. Response to sinusoidal stimulation and dynamics of peripheral vestibular system. J. Neurophysiol. *34*, 661–675.

Fernandez, C., and Goldberg, J.M. (1976a). Physiology of peripheral neurons innervating otolith organs of the squirrel monkey. I. Response to static tilts and to long-duration centrifugal force. J. Neurophysiol. *39*, 970–984.

Fernandez, C., and Goldberg, J.M. (1976b). Physiology of peripheral neurons innervating otolith organs of the squirrel monkey. III. Response dynamics. J. Neurophysiol. *39*, 996–1008.

Fitzpatrick, R.C., Butler, J.E., and Day, B.L. (2006). Resolving head rotation for human bipedalism. Curr. Biol. *16*, 1509–1514.

Fushiki, H., and Barmack, N.H. (1997). Topography and reciprocal activity of cerebellar Purkinje cells in the uvula-nodulus modulated by vestibular stimulation. J. Neurophysiol. *78*, 3083–3094.

Glasauer, S. (1995). Linear acceleration perception: Frequency dependence of the hilltop illusion. Acta Otolaryngol. Suppl. *520*, 37–40.

Glasauer, S., and Merfeld, D.M. (1997). Modeling three-dimensional responses during complex motion stimulation. In Three-Dimensional Kinematics of Eye, Head and Limb Movements, M. Fetter, T. Haslwanter, H. Misslisch, and D. Tweed, eds. (Amsterdam: Harwood Academic Press), pp. 387–398.

Goldberg, J.M., and Fernandez, C. (1975). Vestibular mechanisms. Annu. Rev. Physiol. *37*, 129–162.

Graybiel, A. (1952). Oculogravic illusion. AMA Arch. Ophthalmol. *48*, 605–615.

Graybiel, A., Johnson, W.H., Money, K.E., Malcolm, R.E., and Jennings, G.L. (1979). Oculogravic illusion in response to straight-ahead acceleration of CF-104 aircraft. Aviat. Space Environ. Med. *50*, 382–386.

Green, A.M., and Angelaki, D.E. (2003). Resolution of sensory ambiguities for gaze stabilization requires a second neural integrator. J. Neurosci. *23*, 9265–9275.

Green, A.M., and Angelaki, D.E. (2004). An integrative neural network for detecting inertial motion and head orientation. J. Neurophysiol. *92*, 905–925.

Green, A.M., Shaikh, A.G., and Angelaki, D.E. (2005). Sensory vestibular contributions to constructing internal models of self-motion. J. Neural. Eng. *2*, 164–179.

Guedry, F.E. (1974). Psychophysics of vestibular sensation. In Handbook of Sensory Physiology: The Vestibular System, Part 2, Psychophysics, Applied Aspects and General Interpretations, H.H. Kornhuber, ed. (Berlin: Springer Press), pp. 1–154.

Heinen, S.J., Oh, D.K., and Keller, E.L. (1992). Characteristics of nystagmus evoked by electrical stimulation of the uvular/nodular lobules of the cerebellum in monkey. J. Vestib. Res. *2*, 235–245.

Howard, I.P. (1986). The perception of posture, self-motion and the visual vertical. In Handbook of Perception and Human Performance, K.R. Boff, L. Kaufman, and J.P. Thomas, eds. (New York: Wiley Press), pp. 1–50.

Howard, I.P., and Hu, G. (2001). Visually induced reorientation illusions. Perception *30*, 583–600.

Kano, M., Kano, M.S., Kusunoki, M., and Maekawa, K. (1990a). Nature of optokinetic response and zonal organization of climbing fiber afferents in the vestibulocerebellum of the pigmented rabbit. II. The nodulus. Exp. Brain Res. *80*, 238–251.

Kano, M.S., Kano, M., and Maekawa, K. (1990b). Receptive field organization of climbing fiber afferents responding to optokinetic stimulation in the cerebellar nodulus and flocculus of the pigmented rabbit. Exp. Brain Res. *82*, 499–512.

Kano, M., Kano, M.S., and Maekawa, K. (1991). Simple spike modulation of Purkinje cells in the cerebellar nodulus of the pigmented rabbit to optokinetic stimulation. Neurosci. Lett. *128*, 101–104.

Kaptein, R.G., and Van Gisbergen, J.A. (2006). Canal and otolith contributions to visual orientation constancy during sinusoidal roll rotation. J. Neurophysiol. *95*, 1936–1948.

Marini, G., Provini, L., and Rosina, A. (1975). Macular input to the cerebellar nodulus. Brain Res. *99*, 367–371.

Mayne, R.A. (1974). A system concept of the vestibular organs. In Handbook of Sensory Physiology: Vestibular System, H.H. Kornhuber, ed. (New York: Springer), pp. 493–580.

McNeilage, P.R., Banks, M.S., Berger, D.R., and Buelthoff, H.H. (2007). A Bayesian model of the disambiguation of gravitoinertial force by visual cues. Exp. Brain Res., in press.

Merfeld, D.M. (1995). Modeling the vestibular-ocular reflex of the squirrel monkey during eccentric rotation and roll tilt. Exp. Brain Res. *106*, 123–134.

Merfeld, D.M., and Zupan, L.H. (2002). Neural processing of gravitoinertial cues in humans. III. Modeling tilt and translation responses. J. Neurophysiol. *87*, 819–833.

Merfeld, D.M., Park, S., Gianna-Poulin, C., Black, F.O., and Wood, S. (2005a). Vestibular perception and action employ qualitatively different mechanisms. I. Frequency response of VOR and perceptual responses during Translation and Tilt. J. Neurophysiol. *94*, 186–198.

Merfeld, D.M., Park, S., Gianna-Poulin, C., Black, F.O., and Wood, S. (2005b). Vestibular perception and action employ qualitatively different mechanisms. II. VOR and perceptual responses during combined Tilt andTranslation. J. Neurophysiol. *94*, 199–205.

Mergner, T., and Glasauer, S. (1999). A simple model of vestibular canal-otolith signal fusion. Ann. N Y Acad. Sci. *871*, 430–434.

Musallam, S., and Tomlinson, R.D. (2002). Asymmetric integration recorded from vestibular-only cells in response to position transients. J. Neurophysiol. *88*, 2104–2113.

Naito, Y., Newman, A., Lee, W.S., Beykirch, K., and Honrubia, V. (1995). Projections of the individual vestibular end-organs in the brain stem of the squirrel monkey. Hear. Res. *87*, 141–155.

Newlands, S.D., Vrabec, J.T., Purcell, I.M., Stewart, C.M., Zomerman, B.E., and Perachio, A.A. (2003). Central projections of the saccular and utricular nerves in macaques. J. Comp. Neurol. *466*, 31–47.

Ono, S., Kushiro, K., Zakir, M., Meng, H., Sato, H., and Uchino, Y. (2000). Properties of utricular and saccular nerve-activated vestibulocerebellar neurons in cats. Exp. Brain Res. *134*, 1–8.

Precht, W., Volkind, R., Maeda, M., and Giretti, M.L. (1976). The effects of stimulating the cerebellar nodulus in the cat on the responses of vestibular neurons. Neuroscience *1*, 301–312.

Seidman, S.H., Telford, L., and Paige, G.D. (1998). Tilt perception during dynamic linear acceleration. Exp. Brain Res. *119*, 307–314.

Shaikh, A.G., Green, A.M., Ghasia, F.F., Newlands, S.D., Dickman, J.D., and Angelaki, D.E. (2005a). Sensory convergence solves a motion ambiguity problem. Curr. Biol. *15*, 1657–1662.

Shaikh, A.G., Ghasia, F.F., Dickman, J.D., and Angelaki, D.E. (2005b). Properties of cerebellar fastigial neurons during translation, rotation, and eye movements. J. Neurophysiol. *93*, 853–863.

Smith, M.A., Majaj, N.J., and Movshon, J.A. (2005). Dynamics of motion signaling by neurons in macaque area MT. Nat. Neurosci. *8*, 220–228.

Solomon, D., and Cohen, B. (1994). Stimulation of the nodulus and uvula discharges velocity storage in the vestibulo-ocular reflex. Exp. Brain Res. *102*, 57–68.

Stockwell, C.W., and Guedry, F.E., Jr. (1970). The effect of semicircular canal stimulation during tilting on the subsequent perception of the visual vertical. Acta Otolaryngol. *70*, 170–175.

Tormes, F.R., and Guedry, F.E., Jr. (1975). Disorientation phenomena in naval helicopter pilots. Aviat. Space Environ. Med. *46*, 387–393.

Van Pelt, S., Van Gisbergen, J.A., and Medendorp, W.P. (2005). Visuospatial memory computations during whole-body rotations in roll. J. Neurophysiol. *94*, 1432–1442.

Walberg, F., Pompeiano, O., Brodal, A., and Jansen, J. (1962). The fastigiovestibular projection in the cat. An experimental study with silver impregnation methods. J. Comp. Neurol. *118*, 49–75.

Wearne, S., Raphan, T., and Cohen, B. (1998). Control of spatial orientation of the angular vestibuloocular reflex by the nodulus and uvula. J. Neurophysiol. *79*, 2690–2715.

Wiest, G., Deecke, L., Trattnig, S., and Mueller, C. (1999). Abolished tilt suppression of the vestibulo-ocular reflex caused by a selective uvulonodular lesion. Neurology *52*, 417–419.

Wylie, D.R., De Zeeuw, C.I., DiGiorgi, P.L., and Simpson, J.I. (1994). Projections of individual Purkinje cells of identified zones in the ventral nodulus to the vestibular and cerebellar nuclei in the rabbit. J. Comp. Neurol. *349*, 448–463.

Xiong, G., and Matsushita, M. (2000). Connections of Purkinje cell axons of lobule X with vestibulocerebellar neurons projecting to lobule X or IX in the rat. Exp. Brain Res. *133*, 219–228.

Young, L.R. (1984). Perceptions of the body in space: mechanisms. In Handbook of Physiology: The Nervous System III, I. Darian-Smith, ed. (Bethesda, MD: American Physiological Society Press), pp. 1023–1066.

Zupan, L.H., and Merfeld, D.M. (2003). Neural processing of gravitoinertial cues in humans. IV. Influence of visual rotational cues during roll optokinetic stimuli. J. Neurophysiol. *89*, 390–400.

Zupan, L.H., Merfeld, D.M., and Darlot, C. (2002). Using sensory weighting to model the influence of canal, otolith and visual cues on spatial orientation and eye movements. Biol. Cybern. *86*, 209–230.